Journal of Solar Energy Research (JSER)

Journal homepage: www.jser.ut.ac.ir

Experimental Investigation of Flexible Solar Cells Using Passive Cooling Technique in Hot and Dry Climate of Jodhpur

Lalit Jyani[a*], Sunil Kumar Sankhala[b], Kailash Chaudhary[a] and Kamlesh Purohit[a]

[a] *Department of Mechanical Engineering, MBM University, Jodhpur 342001, India.*
[b] *Defence Laboratory, DRDO Jodhpur 342011, India.*

ARTICLE INFO

Article Type:

Research Article

Received:26.01.2024
Accepted:16.07.2024

Keywords:
Photovoltaic flexible module
Nanomaterial coating
Polyethylene transparent acrylic sheet
Passive cooling.
Heat resistant coating

A B S T R A C T

High temperature is one the important factor that degrades efficiency of Photovoltaic Panels. For every degree increase in the PV temperature, the efficiency decreases by 0.45-0.65%. The Enhancement of performance of flexible PV panel using passive cooling Technique is the main goal of this study. The research aims to optimize the power conversion efficiency of flexible PV panels which are highly affected due to direct contact of mounting surface making them overheat, resulting in decreased output and lifespan. In the present study, two Identical Flexible PV panels 6W each were tested at optimum tilt angle of 31° in atmospheric condition in hot and dry climate of Jodhpur (26.2697°N,73.0352°E), India. Here different electrical parameters of passively cooled panel using Nanomaterial based heat resistant coating were compared with those of a reference panel that lacked cooling. Also, temperature variations over the PV modules were meticulously recorded during August, September, and October using temperature sensors, while considering influencing factors such as wind speed and solar irradiation. According to Experimentation's finding, a temperature reduction of 6-7°C and an improved solar power efficiency of 2.5-4 % were observed for cooled flexible solar panel.

1. Introduction

1.1 Effect of temperature on PV solar cells

The operating temperature is an essential component that influences the efficiency of photovoltaic solar cells. The rising temperature of the solar cell affects the current and voltage. The I-V curve of solar panels demonstrates that the current and voltage vary linearly with temperature [1]. An Increase in solar cell temperature of approximately 1°C causes an efficiency decrease of about 0.45-0.65% [2]. A similar effect occurs in flexible solar cells, which are very sensitive to temperature rise. As a result, lowering the solar cell temperature can immediately improve its efficiency and overall life.

*Corresponding Author Email:jyani.lalit809@gmail.com

Cite this article: Jyani, L., Sankhala, S., Chaudhary, K., & Purohit, K. (2024). Experimental Investigation of Flexible Solar Cells Using Passive Cooling Technique in Hot and Dry Climate of Jodhpur. Journal of Solar Energy Research, 9(2), 1854-1869. doi: 10.22059/jser.2024.371686.1376

DOI: 10.22059/jser.2024.371686.1376

The previously conducted research has extensively investigated the cooling of Rigid Photovoltaic solar cells , with a focus on methods such as active cooling [3], which involves additional bulkiness and moving parts. However, the drawbacks associated with active cooling, including increased weight and complexity, highlight a research gap in the search for alternative cooling techniques. To address this gap, there is a need for exploration into passive cooling methods for flexible Photovoltaic panels which are highly effected by hot climates that effectively reduce solar cell temperatures without compromising on weight and simplicity [3].

1.2 Literature Survey

Several researchers have worked on cooling of PV panels via different approaches, including both active and passive cooling techniques. Air circulation is one of the simplest and natural methods for cooling solar cells, and to enhance convective heat transfer. Edenburn and Edenburn [4] developed a device made up of linear fins fitted on all available heat sink surfaces that is used for passive cooling of cells. Similarly Araki et al. [5] worked on passive cooling technologies for solar cells and reported that good thermal conduction between cells and heat spreading plates was important.

Tonui and Tripanagnostopoulos [6] and Kalogirou [7] reported their experiments on modified PV/T collectors, and the results showed that maximum temperature reduction can be achieved by natural and forced ventilation. As a cooling media, water in different forms has been widely used for PV cooling and is suitable for PV/T systems.

Tripanagnostopoulos et al. [8] compared the electrical efficiency of PV/water, PV/air, and PV/free systems and of PV/insulation under an ambient air temperature of 29°C. It was concluded that a maximum efficiency increase of 3.2% was achieved with PV/water.

Krauter [9] investigated the method of cooling PV modules with a water film flowing on the top surface. With the additional evaporative heat transfer, it was claimed that they could decrease the cell temperature up to 22°C and obtain a net increase in electrical efficiency from 8 to 9%.

Hadipour et al. [10] and Kordzadeh [11] studied the use of water spray to cool PV panels and achieved an increase in the efficiency of solar cells.

Cuse et al. [12] experimentally studied polycrystalline PV cells under controlled conditions in which the illumination was varied from 200 to 800 W/m^2. He used two PV cells, one with aluminum fins as a heat sink and the other without a heat sink. A relative increase in electric efficiency of 9% was observed via the use of passive cooling with a heat sink.

Mazón-Hernández et al.[13] showed that the depth of the air channel between PV cells and roofs has a significant influence on cooling, and the PV module temperature difference is 5-6°C when compared with that of a PV module on a regular mount. Hassan [14], Maiti et al. [15], Smith et al. [16], Rosa-Clot et al. [17] and Elseesy et al. [18] showed that with the right type of PCM material, a decrease in the temperature relative to the reference PV cell can be achieved. The power gain was greater than that of the reference PV module.

Rosa-Clot et al. [17] used a submerged technique to cool down a monocrystalline PV module with water.

El-Seesy et al. [18] attempted to cool PV cells via the thermosyphon effect. The increase in relative efficiency was 19%.

Chandrasekar et al. [19] and Alami [20] used the capillary effect to cool down the back of a monocrystalline PV module with a 0.36 m^2 surface area. The capillary effect was produced via cotton wick structures wrapped spirally at the back of the module and immersed in the fluid. The maximum increase in efficiency reaches 10.4% when compared to that of a noncooled module .

Han et al. [21]compared the cooling of CPV solar cells operated in deionized (DI) water, isopropyl alcohol (IPA), dimethyl silicon oil, and ethyl acetate. In the experiment, an increase in efficiency of 8.5–15.2% was achieved.

Abdulgafar et al. [22] studied the efficiencies of 0.12 W and 15 cm^2 polycrystalline PV cells immersed in deionized water at different depths. An increase in efficiency was observed with increasing water depth, with a maximum value for an efficiency of approximately 22% occurring at a depth of 6 cm.

Lu et al. [23] designed and fabricated ultrabroadband texture imprinted glass to silicon PV modules. Optical tests demonstrated that the silica texture exhibited a higher transmittance within the visible-near infrared wavelength compared to commonly used glass, which improved the effective optical efficiency of solar cells by 5.12% and correspondingly improved the electrical efficiency.

Zhou et al. [24] demonstrated enhanced radiative cooling for low-bandgap PV cells and showed that the operating temperature of solar cells was passively reduced by 10°C, corresponding to a relative open-circuit voltage improvement of 5.7%.

Hashemian and Noorpoor [25] proposed hybrid method of cooling. This integrated system aims to address cooling needs through a dual effect cooling system and heating requirements through a steam Rankine cycle heat exchanger.

Agyekum et al. [26] evaluated the impact of simultaneous dual surface cooling on the PV module's output performance experimentally. The PV module's rear surface was cooled using cotton wick mesh which absorbs water from a perforated pipe and use capillary action to transfer the water down the surface of the rear side of the module and a perforated pipe was used to circulate the water in front surface also.

Dida et al. [27] investigated, a passive cooling system which was developed to mitigate the overheating of PV modules in order to enhance their performance. The developed cooling system is based on water evaporation and the capillary action of the burlap cloth that was attached directly to the rear surface of the module.

Nazari and Eslami [28] demonstrated a three-dimensional computational fluid dynamics (CFD) simulation for forced (wind velocity of 4 m/s) and natural convection (zero wind velocity). Results showed that the perforations are effective in case of natural convection, in which a 3.8 K temperature drop is observed in the best case.

Ozcan et al. [29] studied to achieve cooling effect using an air duct placed under a photovoltaic panel to increase its efficiency. Hourly electricity generation, PV efficiency and cell temperature values were calculated for period of one year using annual temperature and radiation data by using MATLAB and PV Sol software. Maximum cell temperature for the uncooled case is determined as 57.91 °C on July 21st at 1p.m. as a result of hourly calculations.

Yadav and Chandel [30] investigated finding of optimum tilt angle for installation of optimized solar photovoltaic system in India. The optimization of tilt angles is performed using measured solar radiation data for 26 cities in India.

Lee et al. [31] firstly proposes a de-coupled photovoltaic-thermal (PVT) system with solar radiation spectrum-controlled emulsion filter. This system selectively absorbs and transmits solar irradiance to PV module through a liquid filter placed on top of the module, which is named a de-coupled PVT system. The emulsion filter showed a thermal stability up to 70°C and lowered the temperature of the PV module from 46.7°C to 33.1 °C.

Yan et al. [32] demonstrated a strategy for the all season passive thermal modulation enabled by its three-mode functionality of radiative cooling, selective solar absorption, and thermal retention in a scalable manner.

Zhou et al. [33] investigated a passive PV module cooling technique by attaching vortex generators (VGs) on the rear surface of PV modules

Sharaf et al. [34] reviewed various cooling technique to enhance the performance of Photovoltaic Solar cell. The various cooling technique is shown in Table 1 and Figure. 1.

Table.1 Literature review of various cooling technique [34]

Cooling technique	PV surface temperature (^{o}C)	Mainten -ance cost	Heat transfer rate	Life
Forced air	20:30	High	High	Lower life
Forced water	20:30	High	High	Lower then forced air circulation
PV/T Thermal system	20:30	High	High	Similar to forced water
Natural air	50:70	Zero	Low	Longer life
Natural water	30:45	Low	High	Lower
Heat pipe	30:96	Low	High	Longer life

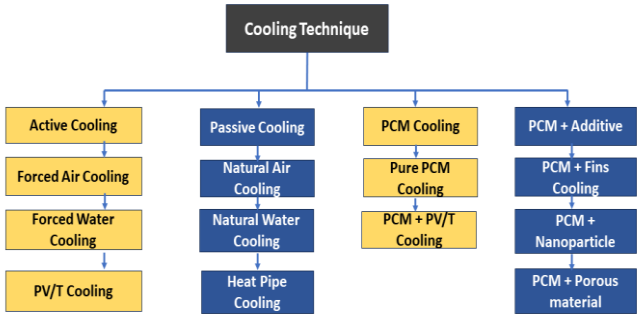

Figure 1: Classification of various cooling technique[34]

There has been many work done by researcher to solve cooling problem in rigid PV solar cell, However there has been no work done for passive cooling of flexible solar cells using nanomaterial coating till date ,the target of this study are:

- The research aims to explore passive cooling techniques for flexible solar cells utilizing nanomaterial based coatings. This involves conducting experiments to assess the efficiency of these coatings in reducing temperature levels and enhancing energy conversion efficiency.
- The experimental procedure entails characterizing the thermal properties of the coatings, monitoring temperature variations across the solar cells under different

environmental conditions, and evaluating the consequential impact on energy conversion efficiency, particularly at the optimum tilt angle.

- Furthermore, the investigation seeks to elucidate the correlation between the application of cool coatings and the resulting temperature and electrical efficiency of flexible solar cells. By scrutinizing these parameters, the study aims to discern the potential benefits of employing nanomaterial-based coatings for passive cooling purposes.

  In summary, the novelty of this research lies in the integration of flexible solar cell technology with nanomaterial-based coatings for passive cooling. This innovative approach holds promise for bolstering the efficiency and longevity of solar energy harvesting systems across diverse applications

2. Material and Methods

2.1 Experimental setup

The experimental setup consists of a 4-cell flexible solar panel with a wattage of 6W, with the cells connected in series, as illustrated in Figure 2. The solar panel is tilted at a 31° angle [35] to maximize radiation at 26.2697°N and 73.0352°E. A roller was used to apply two coatings of silver nanomaterial coating to the acrylic sheet, each 1.5 mils (38 microns approx.) thick. Each coating's thickness was measured using the Positest DFT dry film thickness gauge. Figure 3 depicts the dimensions of both solar panels, which measure 52.5 cm × 13.5 cm.

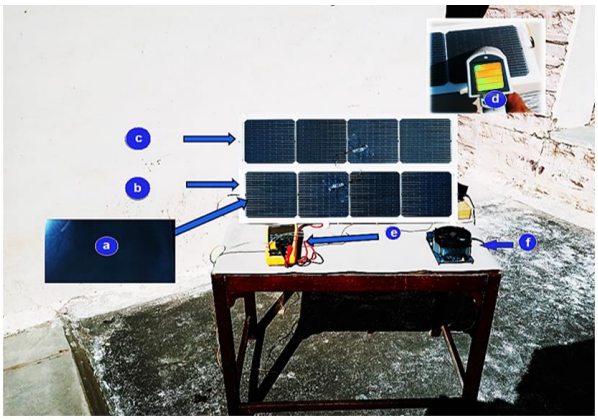

Figure 2. Actual Flexible PV Setup (a) Transparent thin film, (b) flexible solar panel (with coated transparent thin film), (c) flexible solar panel (without coated transparent thin film), and (d) Thermal camera (fluke)) (e). Multimeter (DM 97) (f) Load Circuit

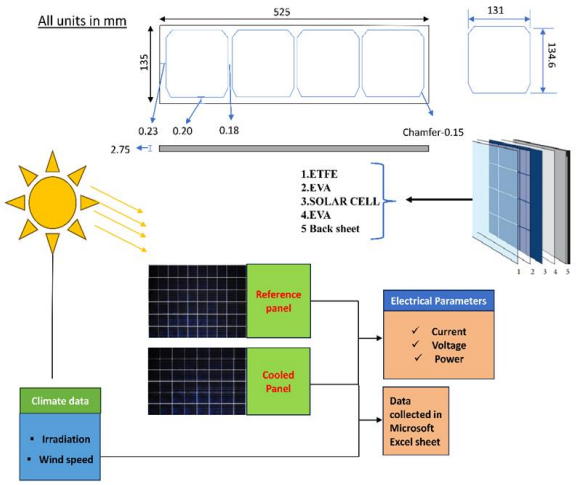

Figure 3. The systematic layout of the experimental setup

2.1.1 Optimum Tilt angle

In this paper, the optimization of the tilt angle for maximum Solar radiation has been estimated for latitude and longitude of Jodhpur. For the estimation, global Solar radiation data of the Indian Meteorological Department (IMD) have been used at different tilt angle to develop a polynomial relationship between the Solar radiation and tilt angle [35]. The obtained tilt angles are compared with those given by others. The highest tilt angle was calculated for month of August, September and October, followed by the evaluation of the average tilt angle to get the optimum value.

2.2 Specification of Data Collection Instruments

The main features of the instruments used in the installation are shown in Table 2. The PV panel temperatures are measured with an IR temperature thermometer and flexible resistance temperature detectors (RTD), which are attached to the front of the panel (panel 1 i.e. Reference panel, panel 2 i.e. cooled panel). Also, load circuit, multimeter, pyranometer and other instruments were used for data collection with minimal error.

2.3 Preparation of the coating

In this study, we applied a silver based heat resistant coating to acrylic sheets with transparency of 82% [36] and thickness of 0.25mm. By using a 7-inch bubble pattern sponge roller we ensured uniform coverage and optimal adhesion. A second coating, applied after 6 hours, aimed to enhance durability. After drying, thickness was measured precisely. The acrylic sheets before and after coating are shown in Figure 4a and Figure 4b, respectively.

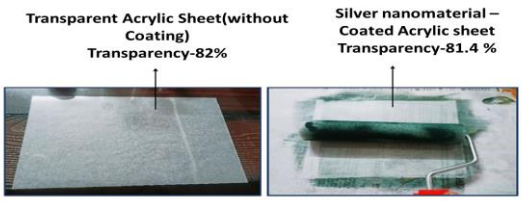

Figure 4. a) A transparent acrylic sheet, 0.25 mm thick. b) Application of a silver based heat resistant coating using a sponge bubble patterned roller, placed over biodegradable paper

2.4 Transmittance of coating

After calibrating the UV-VIS-NIR Cary 5000 spectrophotometer, transparency measurements of an acrylic sheet were conducted across a wavelength range of 450 to 1500 nm. Before and after coating, minimal change in transmittance was observed in the visible spectrum. Post-coating, a transmittance of 81.4% was recorded, indicating effective preservation of transparency. Notably, a decrease in transmittance was observed in the infrared (IR) region. This reduction signifies the coating's successful performance in the IR range, where low transmittance and high reflectance are crucial. This efficacy in the IR spectrum is particularly significant as it helps mitigate the detrimental effects of IR radiation on solar cell performance, thereby contributing to enhanced operational efficiency.

2.5 Characteristics of the nanocoating and instruments used in the experiment

2.5.1 Low-emissivity nanocoating

Low-e coatings are designed to have a high reflectance in the solar spectrum, meaning they reflect a significant portion of the sunlight incident on the PV panel. This reduces the amount of solar radiation absorbed by the panel, thereby minimizing heat gain. In this study, low-emissivity (low-e) coatings are found to reflect solar radiation, exhibiting a reduced emissivity within the infrared spectrum. This characteristic renders them less proficient at radiating heat away from the panel in comparison to the panel without any coating. Consequently, they retain less heat within the panel structure, thereby facilitating passive cooling [37]. A blackbody would have an emissivity of 100%, and a perfect reflector would have a zero value. The emissivity of the surface of a material is its effectiveness in emitting energy as thermal radiation. The typical emissivity of common materials is listed below in Table 3.

Table 2. Description and specification of instruments used in Experimentation

Parameters	Values
Thermal camera (fluke VT-08)	
Temperature range	–20°C to +120°C
Resolution	320 X 340 pixels
Thermal sensitivity	< 0.05°C @ +30°C/50 mK
Measuring accuracy	±2°C or ±2% of reading
Electronic Load(cool master 150)	
Range	0–100 V /0–10 A
Accuracy	±5 mV ±5.4 mA
Multimeter-HTC (with temperature sensor)	
Accuracy	(23±5)^{o}C
Ac Current	± (1.5%10)
AC voltage (true RMS)	± (1.0%+5) for 400 mV ± (0.8%=10d) for 4V,40V,400V
Frequency	± (0.4%+4)
Temperature range	+ 40^{o}C~1000^{o}C
Temperature accuracy	< 400^{o}C ± (0.8%+4) > 400^{o}C ± (1.5%+15)
Pyranometer	
Make	EKO MV-01
Power consumption	9W
Operating temperature range	-30-60^{o}C
Induced Zero offsets	< 1 W/m^2
Maximum operational irradiance	4000 W/m^2
Response time (95%)	< 0.5s

Table 3. The emissivity of materials [37]

S.No	Materials surface	Thermal emissivity
1	Aluminium foil	0.03
2	Asphalt	0.88
3	Brick	0.9
4	Concrete, rough	0.91
5	Glass, smooth (uncoated)	0.91
6	Limestone	0.92
7	Marble, Polished, or white	0.89–0.92
8	Marble, Smooth	0.56
9	Paper, roofing, or white	0.88–0.86
10	Plaster, rough	0.89
11	Silver, polished	0.02
12	Silver Nanomaterial Coating	0.0035

Heat Resistant coating, as depicted in Figure. 5 is a silver based low-E coating which effectively shields glass surfaces by selectively filtering out up to 99.9% of harmful UV rays and 80-90% of infrared (IR) rays emitted by the sun, while still permitting the passage of up to 80% of visible light. This innovative nanocoating serves as a low-emissivity (low-E) coating [37], particularly valuable for enhancing energy efficiency in building design. Unlike traditional coatings, this advanced formulation utilizes nanomaterials to achieve superior performance. It actively mitigates the effects of solar radiation, thereby reducing heat buildup on surfaces such as solar panels, consequently preserving their power conversion efficiency.

Figure 5. Silver-based nano-coating [37]

2.6 Instruments

2.6.1. Thermal Camera

A noncontact fluke VT-08 thermal camera shown in Figure 6a. was used to capture the temperature profile of the solar panel. Its features include an optically matched coaxial laser sight system designed to precisely and accurately outline the target measurement area.

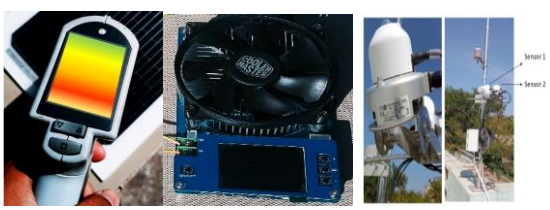

Figure 6. (a) fluke thermal camera (b) Electronic load circuit (c) Pyranometer

2.6.2. Digital Multimeter, Pyranometer and Load Circuit

The current-voltage characteristics of both coated and noncoated solar panels were measured using an HTC DM-97 digital multimeter. Multimeter has an accuracy specified at (23±5)°C and a wide temperature range from +40°C to 1000°C.To apply various loads and plot the current-voltage characteristic curves, a 150W-20A electronic load circuit was utilized. This circuit, depicted in Figure 6b, allowed for the imposition of different loads on the panels, simulating real world conditions. Solar radiation data was collected using an eko MV-01 pyranometer, illustrated in Figure 6c. Pyranometers like this one measure the total solar irradiance received by a surface, providing crucial data for understanding the panels performance under varying levels of solar radiation. In summary, the experiment involved measuring current-voltage characteristics with the digital multimeter, applying loads using the electronic load circuit, and collecting solar radiation data via the pyranometer. These components together facilitated a comprehensive analysis of the coated and uncoated panels behaviour under different environmental conditions.

2.7 Experimental procedure

The readings were taken using ASTM standards [38] from 10:30 a.m. to 4:30 p.m. every 15th day for the month of August, September, and October. The instrumental error was considered minimal. A multimeter HTC DM-97 was used to test the panels current and voltage at various time intervals. A Raytek Raynger MX2 infrared thermometer was used to measure surface temperature with and without coating at various time intervals throughout the day and during the months of August and October. Table 4 shows the specifications for flexible PV panels.

Table 4. Flexible PV panel specification at Standard test condition (STC)

Parameters	**Values**	**Parameters**	**Values**
P_{max}	6 W	Short-circuit current I_{SC}	0.91
Voltage at P_{max} (V_{mp})	6.8 V	Voltage Temperature coefficient (V_M)	-0.3%/°C
Current at P_{max} (I_{mp})	0.88 A	Current Temperature coefficient (I_M)	+0.1/ °C
Open-circuit voltage (V_{oc})	7.2 V	Power Temperature coefficient (P_M)	-(5+0.05)/°C

2.7.1 Experimental environment

The experiment was conducted on fifteenth day of August, September and October. The horizontal worldwide radiation on August 15, September 15, and October 15 between 10:30 am to 4:30 pm is depicted in Figure 7. With the exception of a few cloudiness related aberrations in August and September, the curve shows almost the same behaviour. August's solar radiation was somewhat less than September's because of cloud cover and other atmospheric factors. At midday, the radiation intensity reached 700 W/m^2. Additionally, temporal differences were noted as a result of variations in wind speed, which ranged from 7 to 10 km/h.

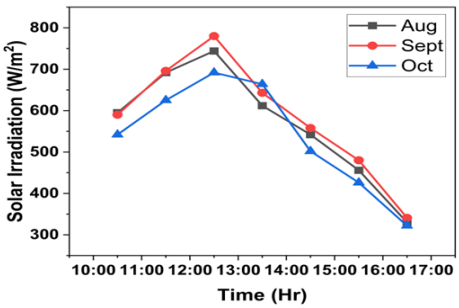

Figure. 7. Irradiation in August, September, and October

2.7.2. Testing condition and assumption

Standard Test Conditions (STC) for photovoltaic solar panels were used for testing and rating their performance. STC assumes ideal conditions with 1000 W/m^2 solar irradiance, representing full solar noon sunshine, a standard air mass (AM) of 1.5, and a cell temperature of 25°C (77°F) [39]. These conditions provided a standardized reference point for comparing solar panel performance. The electrical efficiency η_{ref} (PV) can be calculated at STC. The temperature coefficient β_{ref} is determined by material of PV module. Meanwhile IEC 61215/61646 norms which considers more realistic conditions than STC, defined NOCT as the temperature of a PV module at standard reference environment (SRE: ambient temperature (T_{ambi}) of 20°C, an irradiance of 800 W/m^2, and wind speed of 1 m/s) [40].

2.7.3 Effect of coatings on the temperature of flexible solar cells

Silver based coatings [41] generally keep buildings cool by filtering out UV and infrared rays and transmitting visible rays through windows. Here, the same effect was also seen for flexible solar panels, where a thin transparent film of silver based coating was placed over flexible solar panels. The coating acts as an optical filter, transmits visible light and reflects infrared and ultraviolet radiation, which passively cools the solar panel. The cool coating reduces the temperature of flexible solar cells by controlling the incoming solar radiation, thereby enhancing the overall performance of solar panel.

2.7.4 Electrical Performance

The improvement in Electrical performance of the panel due to the reduction in the temperature can be evaluated by the temperature coefficient of voltage, as shown in Table 4, which is 0.3%/°C [42]. When the temperature of the flexible PV panel decreases, the open-circuit voltage also increases, and vice versa. Figure 10 shows the comparison between cooled panels using a coated thin film and noncooled panels without a coated film. It clearly shows that for the cooled panel, the open-circuit voltage is higher than that for the noncooled panel. The variation in open-circuit voltage is due to variations in atmospheric conditions, i.e., winds and clouds.

The efficiency of solar panels can be calculated by the Evans–Florschuetz PV efficiency correlation [1]

$$\eta_c = \eta_{Tref}[1-\beta_{ref}(T_c - T_{ref})] \quad (1)$$

where η_T is efficiency on module's tilted plane, η_{ref} is the reference efficiency, T_{ref} is the reference temperature of the PV cells, T_{pv} is the temperature of the PV cells, and β is the temperature coefficient of the PV cells based on the data listed in the Evans–Florschuetz thermal model [1]. Here T_{ref} = 25°C, average η_{ref} (PV) = 0.15 and average β_{ref} = (0.0041)^o C^{-1} for c-si were used.

Here, η_{Tref} and β_{ref} are given by the PV manufacturer. The percentage improvement in electrical efficiency is due to passive cooling. The expression for efficiency improvement can be written as [43].

$$\text{Improvement } \% = 100 * \frac{\eta_{\text{cooled PV}} - \eta_{\text{ref PV}}}{\eta_{\text{ref PV}}} \quad (2)$$

Figure 8 shows the ambient air temperature on the same day for August, September, and October. The ambient temperature in September was the highest, exceeding 38°C, while for August and October, it was approximately 37°C at midday. Due to the rainy season in August, where maximum rainfall is

recorded while the temperature does not increase as clouds remain for maximum hours.

2.7.5 Experimental uncertainty assessment

Any experimental activity has the potential to contain some degree of inaccuracy due to measurement or measurand mistakes [44]. In mathematics, the mean, which is represented by x in this case, may be determined using Eq. (3) if there are N observations and x_i designates any of the observations (where i can have any integer value beginning from 1 to N)

$$x = \frac{x_1 + x_2 + \ldots\ldots x_N}{N} = \frac{1}{N}\sum_{i=1}^{N} x_i \qquad (3)$$

Quantitatively evaluating the degree of scatter around the mean for each measurement is crucial in experimental operations. The degree of scatter around the mean value aids in quantifying the random uncertainty by indicating the degree of precision of the experimental data. The most widely used quantitative indicator of dispersion is the standard deviation (SD). When there are equal weight data points, the SD can be computed using Eq. (4) [45].

$$SD = \sqrt{\frac{\sum_{i=1}^{N}(x_i - \bar{x})^2}{N-1}} \qquad (4)$$

The results of the experiment are displayed in Figure 9. From the Figure, it is evident that the uncooled panel's temperature peaked between 12:00 and 1:00 pm. This can be explained by the high outside temperature that was observed during that experimentation period, as seen in Figure 8. The efficiency of the cooling system allowed the cooled panel to retain some degree of temperature stability, nevertheless. However, after 1:30 pm, the temperatures of both panels began to decline because of a sudden reduction in the surrounding air temperature brought on by the appearance of clouds, which also had an impact on the solar radiation intensity. According to the results the cooled system recorded an average temperature of 35.72°C while the uncooled system recorded an average temperature of 59.27°C. The difference in temperature between the two panels averagely is 23.55°C. It can be observed from the Figure that, the temperature of the cooled panel was slightly higher than the uncooled panel at the beginning of the experiment, obviously due to the fact that, the cooled panel was deficient of natural air at the rear side of the panel. As a result, the uncooled panel was being cooled by the ambient air which at the start of the experiment was relatively colder. The SD for the uncooled panel was relatively high compared to the cooled system, the uncooled panel recorded 11.57 against 2.47 for the cooled system. Similarly, the uncertainty for the uncooled system was 3.21 against 0.69 for the cooled system. These large uncertainties can be associated with the sharp rise in the ambient temperature.

The SD provides the estimate for the random uncertainty for any one of the values used in calculating the SD. The SD of the mean value for a number of measurements (σ_m) with equal statistical weights can be calculated using Eq. (5), where the σ_m is the uncertainty [46].

$$\sigma_m = \sqrt{\frac{\sum_{i=1}^{N}(x_i - \bar{x})^2}{N(N-1)}} = \frac{SD}{\sqrt{N}} \qquad (5)$$

3. Results and discussion

3.1 Temperature of the flexible PV panel

Outdoor experiments on flexible solar panels were conducted on every 15th day during the months of August, September and October. The panels, both with and without coating, were tested, and their respective results were recorded along with the panel

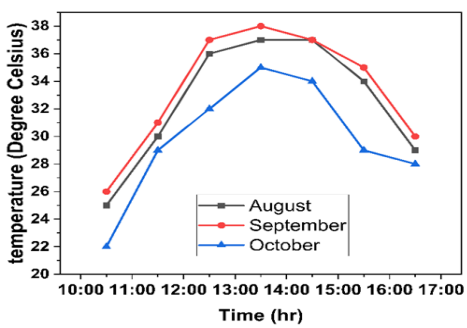

Figure. 8. Ambient temperature in August, September, and October

Temperatures. Figure 9 shows the temperature of flexible solar panels with and without coated acrylic sheets between 10:30 am and 04:30 pm on the 15th of August, September, and October months. The red curve represents the temperature variation for the cooled panel with coating, and the blue curve represents the temperature variation for the panel

without coating. At the start of the experiment, the temperature of both panels increased to a maximum and then started to decrease as the sun's position changed during the day. The minimum temperature is recorded for both panels initially and then start increasing as the sun moves toward the east to west. The temperature of the cooled panel, i.e., the panel with a coated transparent film, is lower than that of the panel without a coated film. The average difference between the two panels is 4°C, and it reaches 6-7°C for some instances.

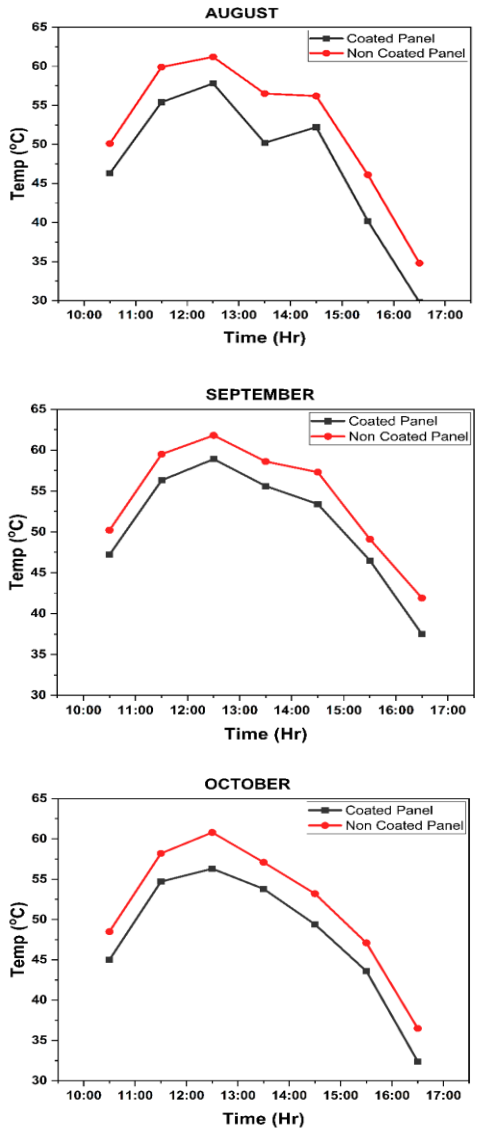

Figure 9. Temperature comparison of two panels in the months of (a) August (b) September (c) October

Table 5. Experimentally calculated values for P_{max}, $I_{max,}$ and V_{max}

Parameters	Modules		Results
	Coated	Non coated	
Pmax	5.05	3.69	% increase in P_{max} = 36.85
Imax	0.78	0.82	% decrease in I_{max} = 4.8
Vmax	6.48	4.50	% increase in V_{max} = 44

3.2 I-V Characteristics of the PV Panel

Figure 10 illustrates the open-circuit voltage and short-circuit current of flexible solar panels with and without coating. Initially, the short-circuit currents of the cooled and noncooled panels are nearly identical. Once the load reaches its peak value and the resistance increases, it subsequently starts to decrease until voltage reaches its maximum and current drops to zero. Table 5 displays the highest current value, or I_{max}, for the coated and noncoated panels, which are 0.78 A and 0.82 A, respectively. The corresponding P_{max} values are 5.05 and 3.69, respectively. For coated panels, the maximum voltage is 6.48 V, while for noncoated panels, it is 4.50V. The aforementioned curve is plotted for August 15th under 744 W/m² of radiation. Similarly for month of September and October with varying light intensities also exhibit similar behaviour as depicted in Figure 10. When the voltage was increased by one unit, the cooled panels efficiency improved by about two percent.

Solar panels output current may marginally increase with temperature. This is because the solar cells charge carriers i.e, their electrons move more freely, producing a higher current production. Similar to this, a solar cells open-circuit voltage usually decreases with temperature. This drop is caused by the increased generation of electron-hole pairs that occur at higher temperatures, which raises leakage current. There is less voltage at the solar cell terminals as a result of this increased leakage current. As a result, these modifications frequently have the net effect of lowering the solar panels total power output. This is due to the fact that a little increase in current usually has a smaller effect on power output than a decrease in voltage. As a result, the cooled panel performs more electrically efficiently than the uncooled panel. Another way to

determine the solar panels efficiency is to use the following formula [42]:

$$\%\,\text{Efficiency} = \left(\frac{\text{Power output of PV cell}}{\text{Power input from sun}}\right)\times 100 \quad (6)$$

$$\%\,\text{Efficiency} = \left(\frac{V_{oc}\times I_{sc}\times \text{fill factor}}{\text{Cell Area}\times 1000}\right)\times 100 \quad (7)$$

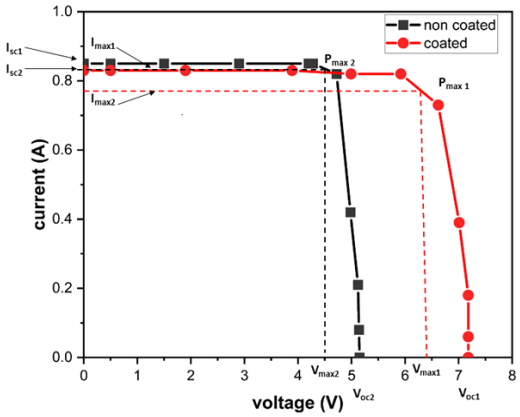

Figure 10. I-V Curve Characteristics for Two Panels for month of August

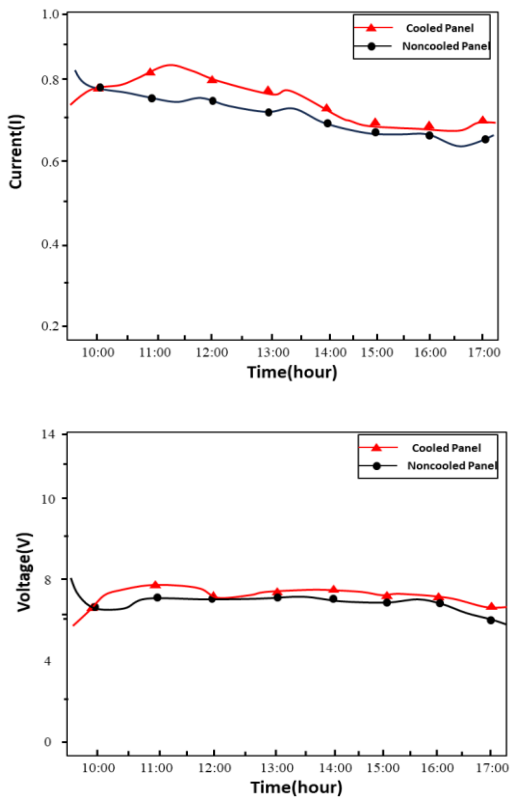

Figure 11. Current and Voltage characteristics of cooled and non-cooled Panel

3.3 Effect on Current and Voltage of the Panel

In Figure 11, the graph illustrating current and voltage clearly indicates that the cooled panel outperforms the non-cooled panel in both cases. The average values of voltage and current for the cooled panel are 7.44 and 0.79, respectively, while for the non-cooled panel, these values are 7.18 and 0.76. This signifies a notable improvement of 3.62% in voltage and a similarly substantial 3.94% improvement in current. These enhancements are evidently attributable to the higher temperature of the uncooled panel. Such improvements in voltage and current are expected to positively influence the efficiency of the panel.

3.4. Thermal characteristics of the panel and weather conditions

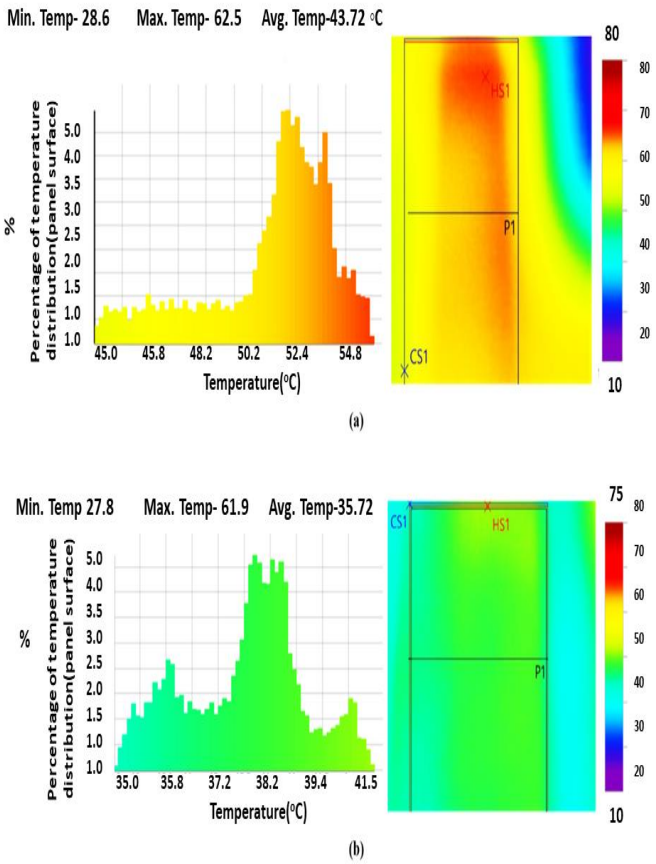

Figure 12. Temperature distribution histogram and thermal images for the (a) uncooled panel (b) cooled panel.

Figures 7 and 8 present data collected at hourly intervals between 10:30 am and 4:30 pm, illustrating solar radiation and ambient temperature. The graph

shows that the maximum solar radiation occurred around 12:30 p.m., normally, this would have occurred at 12 p.m., but due to cloud formation, the mid-day solar radiation was impacted. The average sun irradiation for the day was 582 W/m^2. The daytime average temperature is 28.28^{o}C, with the peak temperature of approximately 37.8^{o}C happening at 1:30 pm.

The temperatures of the two panels were determined by calculating the average of the temperature recorded by each thermocouple placed at the front of the two panels at every 60-minute interval. The findings regarding the temperature distribution during the experiment are shown in Figure 9. The graph shows that in the months of August, September and October the uncooled panel's temperature was maximum between 12:00 and 1:00 pm. This can be explained by the high outside temperature that was observed during that experimentation period, as depicted in Figure 8. The efficiency of the cooling system allowed the cooled panel to retain some degree of temperature stability, nevertheless. However, after 1:30 pm, the temperatures of both panels began to decline because of a sudden reduction in the surrounding air temperature brought on by the appearance of clouds, which also had an impact on the solar radiation intensity. The results showed that the average temperature of the cooled system was 35.72^{o}C, while the average temperature of the uncooled system was 43.27^{o}C. Similarly, at the start of the experiment, the temperature of the cooled panel was marginally higher than that of the uncooled panel. This is most likely because there was not enough natural air on the back side of the cooled panel. As a result, the ambient air, which was initially somewhat colder in the experiment was cooling the uncooled panel. The SD for uncooled panel was relatively higher compared to cooled panel, the uncooled panel SD was recorded 6.57 against 1.38 for the cooled panel. Similarly, the uncertainty for uncooled panel was 1.21 against 0.28 for the cooled panel. The significant increase in the outside temperature after midday and the subsequent decrease in the outside temperature after roughly 2:30 pm can be linked to this significant uncertainty. This resulted to a significant increase in panel temperature, particularly for the uncooled panel, due to which the uncooled panel's SD was on the higher side. Nonetheless, the SD in the cooled panel remained remarkably constant, this is undoubtedly because the cooling system had a significant impact on the PV panel. During the temperature measurement the commonly acknowledged inaccuracy was up to 8%.

When the research findings are compared to the previously studied literature, it becomes clear that the suggested method for cooling the PV system is efficient and capable of significantly lowering the PV panel's temperature in order to improve performance.

The thermal imager was also used to measure the temperature of the panels at around 11:30 a.m. The result for both panel are shown in Figure 12.

It is advisable to conduct this type of examination in sunny weather with a minimum solar irradiance of 600 W/m² [10]. The panel's temperature is graphically represented to illustrate the temperature distribution across its surface. The temperature distribution does not differ appreciably from the thermocouple readings, as indicated by the thermal imager's data. Using the thermal imager, the average temperature of the uncooled panel is 41.28°C, while the thermocouples recorded 43.7°C for the same period. The average temperature of the cooled panel, as measured by the thermal imager, is 37.8°C, whereas the thermocouples recorded 35.72°C.

These variations may result from time differences, meaning that the data for the thermocouples and the thermal imager were not recorded at the same time. Alternatively, it may be the case that the thermocouples are closer in contact compared to thermal imager and can therefore record more accurately. As a result, depending on the surrounding temperature at the moment, timing discrepancies may cause the temperature to gradually increase or decrease. From the thermal image of the cooled panel, it is evident that the panel's temperature distribution is rather uniform. This is probably because the coated sheet was applied evenly throughout the panel. The percentage of temperature distribution on the panel's surface is indicated by the values on the y-axis of the histogram.

3.5. Electrical Efficiency of Panels.

Figure 13 shows the percentage of efficiency gain associated with the temperature change due to passive cooling of the panels by using a low-emissivity coating, which acts as an optical filter that reflects the IR part of the incoming radiation and transmits the visible part.

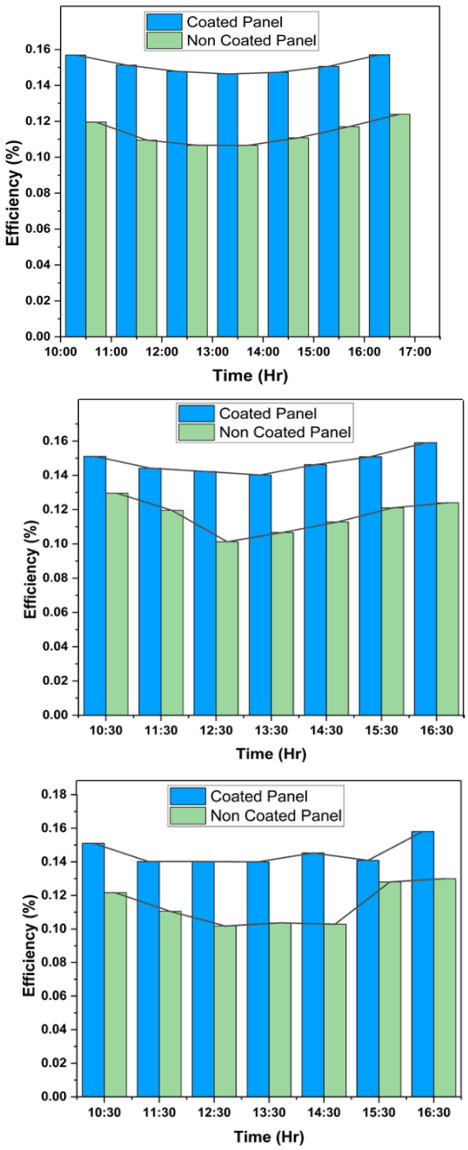

Figure 13. Efficiency comparison for two panels in a month (a) August (b) September (c) October

While mathematical modelling wasn't employed to determine the percentage of reflection and transmission, the coating was found to effectively passively cool the panel. Transmittance was evaluated using a spectrophotometer to assess any reduction resulting from the coating. The temperature variation is greater in August compared to September and October. This is primarily due to August being the rainy season, which results in more frequent and prolonged cloudy conditions throughout the month. In the beginning, the efficiency of both panels decreases and reaches its lowest point at noon as a result of increased losses which increased temperature of the panel. The efficiency started to increase after noon until the readings were recorded. Figure 13 illustrates the average efficiency gains for passively cooled panels in August, September, and October, which are 3.76%, 3.13%, and 3.24%, respectively, compared to non-cooled panels.

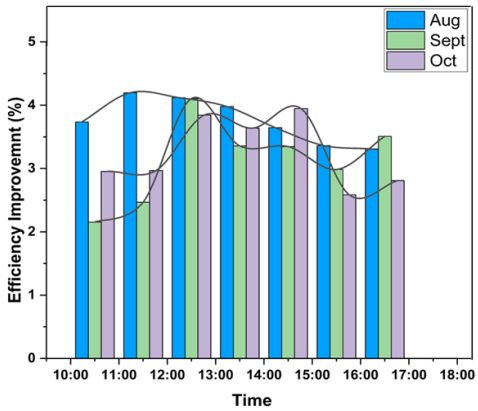

Figure 14. Efficiency improvement in August, September, and October

A comparison of the improvements in efficiency in August, September, and October as shown in Figure 14 revealed that the highest efficiency improvement occurred in August when the value increased by up to 4.19 %. Fluctuations in the curve are observed due to variations in wind speed and seasonal changes occurring in August, September and October.

4. Conclusions

A mechanism to control the temperature of flexible PV panel was proposed in this study. A passive cooling technique was adapted because of its low cost and bulkiness as compared to other technique proposed in literature. This include the use of low emissivity nanomaterial coating on acrylic transparent sheet which was directly placed on Flexible PV panel and results were compared with the Identical panel of same size and specification. The mechanism of cooling can be used for flexible panel due to their low performance compared to Rigid panels and the coating proved to enhance the overall performance of PV panel. The following results were obtained from study.

- In August, the cooled flexible PV panel experienced a substantial reduction in temperature, with the maximum decrease ranging between 6-7°C compared to the noncooled panel.

On average, a decrease of 5°C was observed during this period. Additionally, the passively cooled PV module exhibited a significant increase in electrical efficiency, with the maximum improvement reaching 4.19% compared to the noncooled panel in August.

- It can be concluded that for every increase of 1 volt in average values of I-V characteristics, there is an associated gain in efficiency of up to 2% for the cooled panel.
- Throughout the study period, the open-circuit voltage of the cooled panel consistently rose, consequently boosting the overall power output. Moreover, the cooled panel exhibited commendable stability in its I-V characteristics, marking a notable achievement in competitive performance.
- Improvements in efficiency were consistently observed across August, September, and October for the cooled panel compared to the noncooled counterpart. The peak improvement in efficiency reached 4.19% in August, with an average improvement of 3.76% for that month. Likewise, in September and October, the highest enhancements in electrical efficiency were 4.10% and 3.94%, respectively. The average improvements in electrical efficiency for September and October were 3.13% and 3.24%, respectively.

The results indicate that the low-emissivity coating effectively cools the flexible solar cells while remaining cost effective. The manual application of this thin layer coating proved to be efficient in practice. Furthermore, the reduction in transmittance after coating was minimal, suggesting that the coating had a negligible impact on the overall transparency of the solar cells.

Overall, these findings strongly suggest that the low-emissivity coating enhances the performance of flexible solar cells. By effectively managing temperature without significantly affecting transparency, the coating contributes to improved efficiency and longevity of the solar cells. This underscores the potential of such coatings to enhance the viability and sustainability of solar energy technologies.

Future research endeavors should explore alternative deposition layer techniques and consider the implementation of multilayer coatings to further enhance the overall performance of flexible solar cells. By investigating different deposition methods, such as chemical vapor deposition (CVD), physical vapor deposition (PVD), or spray coating, researchers can optimize the coating process to achieve superior coverage, adhesion, and uniformity on the solar cell surface.

Additionally, the utilization of multilayer coatings offers promising opportunities for enhancing the cooling efficiency and overall performance of flexible PV panels. By combining multiple layers with tailored optical and thermal properties, researchers can optimize the coating's ability to reflect solar radiation while minimizing heat absorption. This approach can lead to more effective temperature management and improved energy conversion efficiency of the solar cells.

Furthermore, future studies should focus on integrating the resulting materials with flexible PV panels during the fabrication process. By incorporating the coated materials directly into the panel manufacturing process, researchers can ensure seamless integration and compatibility with existing production techniques. This would facilitate the widespread adoption of passive cooling technologies in commercial solar panel applications.

Acknowledgements

I acknowledge Defence Laboratory Jodhpur and MBM University Jodhpur who provided me with research facility and kind support throughout my research work. I also Acknowledge my guide for his valuable guidance and support for every step of my research.

Nomenclature

FF	fill factor
STC	standard test condition
V	voltage (V)
I	electric current (A)
η	energy efficiency (%)
T	temperature (K)
T_c	cell module temperature(K)

Greek Letter

β	temperature coefficient (K^{-1})
η	cell/module electrical efficiency (%)
σ	uncertainty

Subscript

ref	reference value, at reference conditions
T	on module's Tilted plane

oc	open circuit
sc	short circuit
c	cell (module)
m	maximum, at maximum power point
cooled	cooled panel
PV	photovoltaic panel

References

[1] Skoplaki, E., & Palyvos, J. A. (2009). On the temperature dependence of photovoltaic module electrical performance: A review of efficiency/power correlations. *Solar energy*, 83(5), 614-624. DOI: 10.1016/j.solener.2008.10.008

[2] Notton, G., Cristofari, C., Mattei, M., & Poggi, P. (2005). Modelling of a double-glass photovoltaic module using finite differences. *Applied thermal engineering*, 25(17-18), 2854-2877.DOI: 10.1016/j.applthermaleng.2005.02.008

[3] Grubišić-Čabo, F., Nižetić, S., & Giuseppe Marco, T. (2016). Photovoltaic panels: A review of the cooling techniques. *Transactions of FAMENA*, 40(SI-1), 63-74. Retrieved from https://hrcak.srce.hr/159196

[4] Edenburn, M. W., & Edenburn, M. W. (1981). Active and passive cooling for concentrating photovoltaic arrays. *NASA STI/Recon Technical Report* N, 82, 21745.

[5] Araki, K., Uozumi, H., & Yamaguchi, M. (2002, May). A simple passive cooling structure and its heat analysis for 500/spl times/concentrator PV module. *In Conference Record of the Twenty-Ninth IEEE Photovoltaic Specialists Conference*, 2002. (pp. 1568-1571). IEEE. DOI: 10.1109/PVSC.2002.1190913

[6] Tonui, J. K., & Tripanagnostopoulos, Y. (2007). Improved PV/T solar collectors with heat extraction by forced or natural air circulation. *Renewable energy*, 32(4), 623-637. DOI: 10.1016/j.renene.2006.03.006

[7] Kalogirou, S. A. (2001). Use of TRNSYS for modelling and simulation of a hybrid pv–thermal solar system for Cyprus. *Renewable energy*, 23(2), 247-260. DOI: 10.1016/S0960-1481(00)00176-2

[8] Tripanagnostopoulos, Y., Nousia, T. H., Souliotis, M., & Yianoulis, P. (2002). Hybrid photovoltaic/thermal solar systems. *Solar energy*, 72(3), 217-234. DOI:10.1016/S0038-092X(01)00096-2

[9] Krauter, S. (2004). Increased electrical yield via water flow over the front of photovoltaic panels. *Solar energy materials and solar cells*, 82(1-2), 131-137.DOI: 10.1016/j.solmat.2004.01.011

[10] Hadipour, A., Zargarabadi, M. R., & Rashidi, S. (2021). An efficient pulsed-spray water cooling system for photovoltaic panels: Experimental study and cost analysis. *Renewable Energy*, 164, 867-875. DOI: 10.1016/j.renene.2020.09.021

[11] Kordzadeh, A. (2010). The effects of nominal power of array and system head on the operation of photovoltaic water pumping set with array surface covered by a film of water. *Renewable energy*, 35(5), 1098-1102. DOI: 10.1016/j.renene.2009.10.024

[12] Cuce, E., Bali, T., & Sekucoglu, S. A. (2011). Effects of passive cooling on performance of silicon photovoltaic cells. *International Journal of Low-Carbon Technologies*, 6(4), 299-308. DOI: 10.1093/ijlct/ctr018

[13] Mazón-Hernández, R., García-Cascales, J. R., Vera-García, F., Káiser, A. S., & Zamora, B. (2013). Improving the electrical parameters of a photovoltaic panel by means of an induced or forced air stream. *International Journal of Photoenergy*, 2013. DOI: 10.1155/2013/830968

[14] Hassan, A. (2010). Phase change materials for thermal regulation of building integrated photovoltaics. *Dissertation*, Technological University Dublin

[15] Maiti, S., Banerjee, S., Vyas, K., Patel, P., & Ghosh, P. K. (2011). Self-regulation of photovoltaic module temperature in V-trough using a metal–wax composite phase change matrix. *Solar energy*, 85(9), 1805-1816. DOI: 10.1016/j.solener.2011.04.021

[16] Smith, C. J., Forster, P. M., & Crook, R. (2014). Global analysis of photovoltaic energy output enhanced by phase change material cooling. *Applied energy*, 126, 21-28. DOI: 10.1016/j.apenergy.2014.03.083

[17] Rosa-Clot, M., Rosa-Clot, P., Tina, G. M., & Scandura, P. F. (2010). Submerged photovoltaic solar panel: SP2. Renewable Energy, 35(8), 1862-1865. DOI: 10.1016/j.renene.2009.10.023

[18] Elseesy, I., Khalil, T., & Ahmed, M. H. (2012). Experimental investigations and developing of photovoltaic/thermal system. *World Applied Sciences Journal*, 19(9), 1342-1347. DOI: 10.5829/idosi.wasj.2012.19.09.2794

[19] Chandrasekar, M., Suresh, S., & Senthilkumar, T. (2013). Passive cooling of standalone flat PV module with cotton wick structures. *Energy conversion and management*, 71, 43-50.DOI: 10.1016/j.enconman.2013.03.012

[20] Alami, A. H. (2014). Effects of evaporative cooling on efficiency of photovoltaic modules. *Energy Conversion and Management*, 77, 668-679. DOI: 10.1016/j.enconman.2013.10.019

[21] Han, X., Wang, Y., & Zhu, L. (2013). The performance and long-term stability of silicon concentrator solar cells immersed in dielectric liquids. *Energy conversion and management*, 66, 189-198. DOI: 10.1016/j.enconman.2012.10.009

[22] Abdulgafar, S. A., Omar, O. S., & Yousif, K. M. (2014). Improving the efficiency of polycrystalline solar panel via water immersion method. *International Journal of Innovative Research in Science, Engineering and Technology*, 3(1), 8127-8132.

[23] Lu, Y., Chen, Z., Ai, L., Zhang, X., Zhang, J., Li, J., & Song, W. (2017). A universal route to realize radiative cooling and light management in photovoltaic modules. *Solar Rrl*, 1(10), 1700084. DOI: 10.1002/solr.201700084.

[24] Zhou, Z., Wang, Z., & Bermel, P. (2019). Radiative cooling for low-bandgap photovoltaics under concentrated sunlight. *Optics express*, 27(8), A404-A418.DOI: 10.1364/OE.27.00A404

[25] Hashemian, N., & Noorpoor, A. (2023). Thermo-eco-environmental Investigation of a Newly Developed Solar/wind Powered Multi-Generation Plant with Hydrogen and Ammonia Production Options. Journal of Solar Energy Research, 8(4), 1728-1737. doi: 10.22059/jser.2024.374028.1388

[26] Agyekum, E. B., PraveenKumar, S., Alwan, N. T., Velkin, V. I., & Shcheklein, S. E. (2021). Effect of dual surface cooling of solar photovoltaic panel on the efficiency of the module: experimental investigation. *Heliyon*, 7(9). DOI: 10.1016/j.heliyon. 2021.e07920.

[27] Dida, M., Boughali, S., Bechki, D., & Bouguettaia, H. (2021). Experimental investigation of a passive cooling system for photovoltaic modules efficiency improvement in hot and arid regions. *Energy Conversion and Management*, 243, 114328. DOI: 10.1016/j.enconman.2021.114328.

[28] Nazari, S., & Eslami, M. (2021). Impact of frame perforations on passive cooling of photovoltaic modules: CFD analysis of various patterns. *Energy Conversion and Management*, 239, 114228.DOI: 10.1016/j.enconman.2021.114228

[29] Özcan, Z., Gülgün, M., Şen, E., Çam, N. Y., & Bilir, L. (2021). Cooling channel effect on photovoltaic panel energy generation. *Solar Energy*, 230, 943-953. DOI: 10.1016/j.solener.2021.10.086

[30] Yadav, A. K., & Chandel, S. S. (2018). Formulation of new correlations in terms of extraterrestrial radiation by optimization of tilt angle for installation of solar photovoltaic systems for maximum power generation: case study of 26 cities in India. *Sādhanā,* 43, 1-15. DOI: 10.1007/s12046-018-0858-2

[31] Lee, J. W., Song, M. S., Jung, H. S., & Kang, Y. T. (2023). Development of solar radiation spectrum-controlled emulsion filter for a photovoltaic-thermal (PVT) system. *Energy Conversion and Management*, 287, 117087.DOI: 10.1016/j.enconman.2023.117087

[32] Yan, C., Li, A., Wu, H., Tong, Z., Qu, J., Sun, W., & Yang, Z. (2023). Scalable and all-season passive thermal modulation enabled by radiative cooling, selective solar absorption, and thermal retention. *Applied Thermal Engineering*, 221, 119707.DOI: 10.1016/j.applthermaleng.2022.119707

[33] Zhou, Z., Gentle, A., Mohsenzadeh, M., Jiang, Y., Keevers, M., & Green, M. (2024). Long-term outdoor testing of vortex generators for passive PV module cooling. *Solar Energy*, 275, 112610.DOI: 10.1016/j.solener.2024.112610

[34] Sharaf, M., Yousef, M.S. & Huzayyin, A.S. Review of cooling techniques used to enhance the efficiency of photovoltaic power systems. *Environmental Science Pollution Research*. 29, 26131–26159 (2022). DOI:10.1007/s11356-022-18719-9

[35] Singh, D., Singh, A. K., Singh, S. P., & Poonia, S. (2021). Optimization of tilt angles for solar devices to gain maximum solar energy in Indian climate. In Advances in Clean Energy Technologies: Select *Proceedings of ICET 2020 (pp. 189-199). Springer Singapore*. DOI:10.1007/978-981-16-0235-1_16

[36] Jorgensen, G. J., Brunold, S., Koehl, M., Nostell, P., Oversloot, H., & Roos, A. (1999, October). Durability testing of antireflection coatings for solar applications. *In Solar Optical Materials XVI* (Vol. 3789, pp. 66-76). SPIE.

DOI: https://doi.org/10.1117/12.367571

[37] Jelle, B. P., Kalnæs, S. E., & Gao, T. (2015). Low-emissivity materials for building applications: A state-of-the-art review and future research perspectives. Energy and Buildings, 96, 329-356. DOI: 10.1016/j.enbuild.2015.03.024

[38] K. Emery, (2007) Standardization News 35(1): 30-33. *Report* URL: https://www.researchgate.net/publication/255945173

[39] Roy, J. N., Gariki, G. R., & Nagalakhsmi, V. (2010). Reference module selection criteria for accurate testing of photovoltaic (PV) panels. *Solar Energy*, 84(1), 32-36. DOI: 10.1016/j.solener.2009.09.007

[40] Photovoltaics, D. G., & Storage, E (2021). IEEE Recommended Practice for Testing the Performance of Stand-Alone Photovoltaic Systems. ,1-32, DOI: 10.1109/IEEESTD.2021.9508826.

[41] Nikitenkov, N. (Ed.). (2017). Modern technologies for creating the thin-film systems and coatings. BoD–Books on Demand (United Kingdom. Intech Open Press) DOI: 10.5772/63326

[42] Hassan, R. (2020, November). Experimental and numerical study on the effect of water cooling on PV panel conversion efficiency. In IOP Conference Series: Materials Science and Engineering (Vol. 928, No. 2, p. 022094). *IOP Publishing*. DOI: 10.1088/1757-899X/928/2/022094

[43] Haidar, Z. A., Orfi, J., & Kaneesamkandi, Z. (2018). Experimental investigation of evaporative cooling for enhancing photovoltaic panels efficiency. *Results in Physics*, 11, 690-697. DOI: 10.1016/j.rinp.2018.10.016

[44] Chandrika, V. S., Karthick, A., Kumar, N. M., Kumar, P. M., Stalin, B., & Ravichandran, M. (2021). Experimental analysis of solar concrete collector for residential buildings. *International Journal of Green Energy*, 18(6), 615-623.DOI: 10.1080/15435075.2021.1875468

[45] Chandel, R. (2013). Uncertainty analysis of photovoltaic power measurements using solar simulators. *Energy Technology*, 1(12), 763-769. DOI: 10.1002/ente.201300112

[46] Naqvi, S. A. R., Kumar, L., Harijan, K., & Sleiti, A. K. (2024). Performance investigation of solar photovoltaic panels using mist nozzles cooling system. *Energy Sources, Part A: Recovery, Utilization, and Environmental Effects*, 46(1), 2299–2317. DOI:10.1080/15567036.2024.2305302